

Effect of Trailing Edge Flaps on Power Coefficient of a Horizontal Axis Wind Turbine Model

Mahmoud Khalil^{1,*}, A. Abd Elmotalip², M.M.Elsakka³, M.El-Gandour⁴

^{1,*} Mechanical Power Engineering Department, Faculty of Engineering, Port Said University, Port Said, Egypt, M.Khalil@eng.psu.edu.eg

²Mechanical Power Engineering Department, Faculty of Engineering, Port Said University, Port Said, Egypt, abdelhadyelabady@gmail.com

³Mechanical Power Engineering Department, Faculty of Engineering, Port Said University, Port Said, Egypt, elsakka@eng.psu.edu.eg

⁴Mechanical Power Engineering Department, Faculty of Engineering, Port Said University, Port Said, Egypt, mghandour@eng.psu.edu.eg

*Corresponding author, DOI: 10.21608/PSERJ.2023.194752.1222,

ABSTRACT

The field of wind energy has made significant progress, yet there is always room for improving efficiency and the energy extracted from horizontal axis wind turbines HAWTs. There is interest in new renewable energies, including wind energy. This study aims to investigate the effect of trailing edge flap on the performance of the turbine at different numbers of blades, different blade angles, and flap angles. Therefore, an experimental setup includes a model of wind turbine was constructed. The performance of a HAWT model with trailing edge flaps added is examined in this research using the findings of wind tunnel tests. A model with two, three, and six-bladed rotors with a diameter of 260 mm was employed for the wind tunnel tests. The wind turbine model is tested at various blade angles and tip speed ratios. The model was initially tested at various blade angles without any flaps, β , of 10°, 15° and 20°, with two, three, and six-bladed rotors and secondly the wind turbine model was tested with additional trailing edge flaps with flap angle, α , of 40°, 50° and 60°. It was found that the use of trailing edge flaps can improve the HAWT performance.

Keywords: Wind Energy, HAWT, Trailing edge Flap, Power Coefficient.

Received 18-2-2023

Revised 26-3-2023

Accepted 30-4-2023

© 2023 by Author(s) and PSERJ.

This is an open access article licensed under the terms of the Creative Commons Attribution International License (CC BY 4.0).
<http://creativecommons.org/licenses/by/4.0/>



1. INTRODUCTION

For human civilization to advance, energy is required. In addition, the global demand of energy is expected to increase due to the ever-increasing population and due to the impressive advancements in a number of areas, including business, transportation, and the economy. For decades, fossil fuels were the main source of energy which emit large amounts of harmful emissions and greenhouse gases (GHG). Eventually, global warming and its subsequent climate change severe impacts, are frequently visible everywhere. To protect our environment, the world seeks alternative energy sources that are environmentally friendly. Among these sources, wind energy is one of the most promising alternative energy sources [1]. It is the second most mature technology to capture power from alternative sources just after hydropower. By the time, wind turbines get bigger and taller to capture as large as possible of wind energy and to reach air with higher velocities. However, these giant turbines are most suitable for rural areas as it can interfere with human activities. Hence, small wind turbines appear to be most suitable for urban areas. There is much research on small horizontal axis wind turbine (SHAWT) both experimental and numerical. As a result of the dominance of the HAWT in the wind turbine industry, more and more attention are now being paid to it. Schubel and Crossley [2] presented a state of art review about wind turbine design. In their review, they included blade plan shape/quantity, airfoil selection and optimal attack angles. They found that an efficient blade shape depends on the performance of the selected airfoils. Widiyanto et al. [3] held an analysis for the performance of a SHAWT with airfoil NACA 4412. The analysis examined wind flow around the airfoil using the integral boundary layer formulation and the potential flow panel approach. Suresh et al. [4] found that the SD7080 airfoil have the best power coefficient for SHAWT at tip speed ratio, λ , = 6 for Reynolds number (Re) = 81712 in numerical simulations, making it the best airfoil to start producing high power in low wind speed applications.

The geometry of the Invelox wind was to increase the air net mass flow rate as it enters the Invelox, increase the wind power at the Venturi's throat, and reduce backflow at the diffuser's outlet [5]. The effect of the modification of the blade tip on the performance of the rotors was studied by Iswahyudi et al. [6]. Kaviani and A. Nejat [7] used a transient two-way partitioned Fluid-Solid interaction technique to analyze the fluid-solid

interaction. Bhavsar et al. [8] improved HAWT aerodynamic performance using a slot design airfoil.

There were several studies that implemented and studied adding flaps at the leading and trailing edges of turbine blades. Using shorter frontal flaps Shehata et al. [9] improved the maximum power coefficient compared to the reference case, and using shorter rear flaps improved the model's maximum power coefficient by 2.5 when compared to the reference case. For the three-bladed rotor model, the maximum power coefficient was 49.6% with an enhancement of 3.33% in power coefficient. This experimental study revealed that employing shorted frontal flaps with a horizontal axis wind turbine model's rotor main blade is preferable in contrast with the use of shorted rear flaps.

Zhuang et al. [10] investigated the potential effects of morphing trailing-edge flaps (MTEF) on the aerodynamic load control of an oscillating airfoil by means of computational simulations. A number of MTEF kinematic control parameters, including deflection length (a), amplitude (β amp), and phase shift (ϕ) has been investigated. In their numerical simulations, a wind turbine rotor with and without the Gurney flap is considered at tip speed ratios of 4.59 and 6.35. Zhang et al. [11] studied the effect of root Gurney flaps on the aerodynamic performance of a horizontal axis wind turbine. Their results show that Gurney flap deployment boosted efficiently the rotor's power coefficients by 21% at $\lambda = 6.35$, according to a comparison of numerical results with experimental observations.

Mansi and Aydin [12] studied the impact of a fixed trailing edge flap on the aerodynamic performance of SHAWT using the blade element momentum (BEM). They proposed a modified blade profile to improve the turbine performance. They found that the modified blade produced better performance when taking into account a three-bladed turbine, compared to the reference profile's power coefficient of 0.355, with a power coefficient of 0.39. In addition, according to 3D CFD research, the enhanced blade's power coefficient was found to be 0.444, which is 14% higher than the power coefficient discovered using BEM. Bofeng et al. [13] analysed the aerodynamic performance of wind turbine using trailing-edge flap. The results showed that the airfoil body's gap with the flap has an impact on the flaps' aerodynamic performance, the vortex and boundary layer separation at

the trailing edge can be successfully reduced by the proposed trailing-edge flaps.

According to the previous literature review, no research has been done on the efficiency increase of HAWTs with the trailing-edge flap at different flap angles. Therefore, the current study investigates experimentally the effect of trailing edge flaps at different setting angles on the performance of the turbine for different numbers of blades.

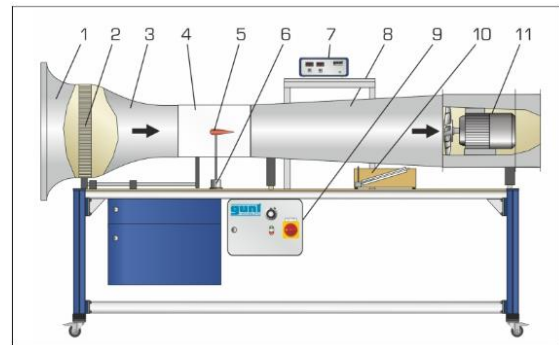
2. EXPERIMENTAL SETUP

The traditional test setup for aerodynamic flow experiments is a wind tunnel. In this study, the open wind displayed and measured in an open wind tunnel. Its technical specifications as shown in Table 1. For this purpose, the air is accelerated after being sucked in from the surroundings. The air flows around the wind turbine model, in the test section. A diffuser is then used to slow down the air and a fan is used to distribute it back into the open air, as shown in Figure 1.

In the closed measuring portion, a homogenous velocity distribution with minimum turbulence is ensured by a flow straightener and a precisely selected nozzle contour. The measurement section's flow cross-section is square. The integrated axial fan stands out for operating with excellent efficiency while using less energy together with an outlet guiding vanes system and variable-speed drive.

Table 1: Technical specifications for HM 170 open wind tunnel

Measuring section	Measuring ranges	Dimensions and weight
<ul style="list-style-type: none"> ▪ Flow cross-section WxH: 292x292 mm ▪ length: 420 mm ▪ wind velocity: 1,3...25 m/s ▪ Axial fan power consumption: 3.4 kW 	<ul style="list-style-type: none"> ▪ force: lift: ±4 N ▪ drag: ±4 N ▪ velocity: 1,3...25 m/s ▪ angle: ±180° 	<ul style="list-style-type: none"> ▪ LxWxH: 2870x890x1540 mm ▪ Weight: approx.250 kg



- | | | | |
|-------------------|----------------------|-----------------|----------------------|
| 1: inlet contour | 2: flow straightener | 3: nozzle | 4: measuring section |
| 5: model | 6: force sensor | 7: control unit | 8: diffuser |
| 9: switch cabinet | 10: manometer | 11: axial fan | |

Figure 1: A photograph of the open return wind tunnel.

Using a rope brake dynamometer, the shaft torques were measured. When used for testing tiny wind turbines in a wind tunnel, the method can produce a good torque value. The device's primary torque measurement mechanism is shown in Figures 2 and 3. The shaft of the tested wind turbine was connected to a metal pulley by a DP-diameter shaft. A rope with its ends attached to a digital weighing scale twisted the pulley. When the rotor was rotating steadily, the digital balance displayed a S (N) value, and the applied torque, T (N m), on the pulley was weighted by W (N), those conditions were met. After that, we could determine the torque by the following Equation.

$$T = (Dp/2) (W - S) \quad (1)$$

Shaft Speed Measurement, the speed of the rotor model was measured by an optical tachometer, and its accuracy of speed reading was ± 5 RPM. Wind speed measurement is carried out using Magnehelic® gauge which is the industry standard to measure air velocity. The measurement was made before the wind turbine model in static pressure port according to Bernoulli's equation. The magnitude of the static pressure on the wind tunnel walls is equivalent to the kinetic head.

The wind turbine model rotor blades are tapered and equipped with Joukowski airfoil-sections as can be seen in Figure 4. The blades were made from PLA+. And they were manufactured with a profile obtained according to the following equations.

$$\eta_1 = 2eb(1 + \cos \varphi) \sin \varphi + 2ab \sin 2\varphi \quad (2)$$

$$\eta_2 = -2eb(1 + \cos \varphi) \sin \varphi + 2ab \sin 2\varphi \quad (3)$$

$$\zeta = 2b \cos \varphi \quad (4)$$

where

$$C = \text{blade chord}, \varphi = \text{airfoil angle} \quad \& \quad \alpha = \eta_{\max} / 2b$$

$$e = T_{\max} / 1.3 C, \quad b = 0.25 C \quad \& \quad T_{\max} = 0.15 C$$

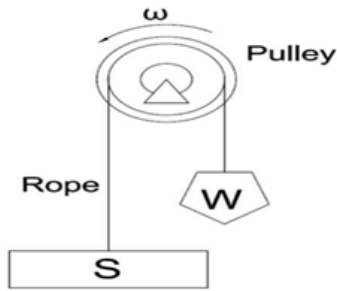


Figure 2: Rope brake dynamometer.

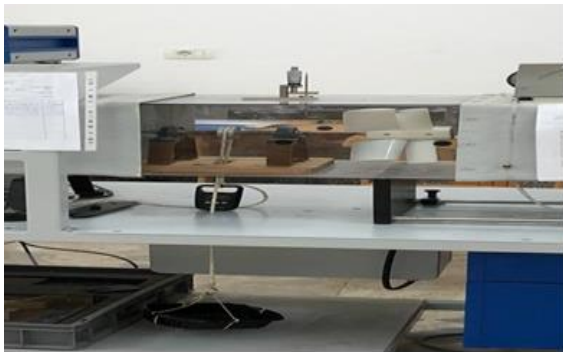


Figure 3: Photograph of rope brake Power method.

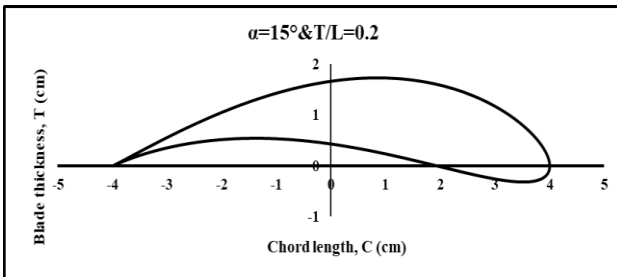


Figure 4: Blade profile based on Joukowski transformation.

Due to its front loading, the NACA 0012 offers an excellent section for the flap and enables the use of the entire flap for the airfoil's pressure recovery as can be seen in Figure 5. The flap angle can be changed to prevent the flap's propensity to create a leading-edge pressure peak.

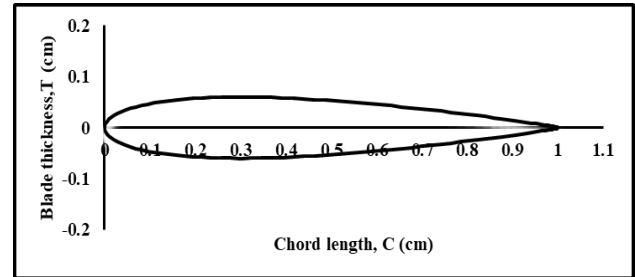


Figure 5: Flap Blade profile based on NACA0012.

There is a type of force operating on the blades of a wind turbine, it is the circumferential force in the direction of turbine rotation that provides the torque. The realizable torque, T_R , from a wind turbine is obtained by:

$$T_R = C_T (1/2) \rho A V^2 r_m \quad (5)$$

$$C_T = T_R / (1/2) \rho A V^2 r_m \quad (6)$$

where

$$r_m = (D/2) \sqrt{[(1 + \lambda^2) / 2]} \quad (7)$$

The power coefficient, C_P is a function of wind turbine rotor characteristics and the working tip speed ratio of the turbine; it can be expressed in the following form.

$$C_P = P_R / (1/2) \rho A V^3 \quad (8)$$

Where, P_R is the realized power from a wind turbine and is obtained as

$$P_R = T_R \omega \quad (9)$$

3. RESULTS AND DISCUSSION

In this section, an attempt is made to present the results obtained from the tests. The experiments can be divided into two parts, first is the preliminary tests which were carried out on the model without flaps at different blade angles, and different numbers of blades while the second part focuses on the model with flaps. All experiments were carried out at a wind speed of 9 m/s, except for six blades rotor that were at 8 m/s. The results are also divided into experimental results describing overall performance and detailed analytical

measurements of the flow. Configurations with and without flaps were also examined, each part will be explained in more details later.

3.1 Reference Configurations Results

3.1.1 Configuration (A)

In this section, the torque coefficient (C_T) against tip-speed ratio (λ) characteristic of a 2-bladed turbine model without Flaps is examined at three different blade angles (10° , 15° , 20°). The torque coefficient is defined as the ratio of measured torque to calculated torque, and the tip speed ratio is defined as the ratio between the blade tip speed to wind speed. Figure 6 shows the relation between the torque coefficient, and tip speed ratio for a blade angles of 10° , 15° , and 20° . It is noticed that, for blade angle of 10° , at a tip speed ratio of 0.412, the torque coefficient is 9.0%. By increasing the ratio of tip speed, the torque coefficient increases until its maximum value of 15.6% at a tip speed ratio of 0.496, then any increase in the tip speed ratio over 0.496 leads to a decrease in the torque coefficient. For the blade angle of 15° , the torque coefficient increased from 10% at a tip speed ratio, λ of 0.42 to its maximum value of 22% at a ratio of tip speed 0.465. It gave an improvement of 41.9% when compared with the corresponding results with a blade angle of 10° . Finally, this configuration tested at blade angle of 20° with the same wind velocity range, and it was found that it achieved a lower performance in contrast with the turbine model with a blade angle of 15° . It gave about 17.3% maximum torque coefficient at a ratio of tip speed 0.481 as shown in Figure 6. The improvement in the maximum torque coefficient, ΔC_T is calculated as follows:

$$\Delta C_T = [C_{T \max @ \beta = 15^\circ} - C_{T \max @ \beta = 10^\circ}] / C_{T \max @ \beta = 10^\circ} (10)$$

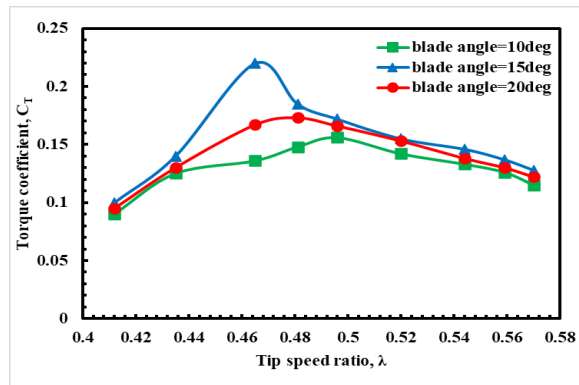


Figure 6: The relation between torque coefficient and tip speed ratio for a two-bladed turbine with blade angles of 10° , 15° , and 20° .

Figure 7 shows the power coefficient (C_P) of the tested 2-bladed model against tip speed ratio at blade angles of 10° , 15° , and 20° . For the blade angle of 10° , the power coefficient increases from 3.8% at tip speed ratio of 0.41 to maximum value of 6% at tip speed ratio of 0.496 and then decreases with increasing in tip speed ratio. It is noticed that the power coefficient increased from 8.4% at tip-speed ratio of 0.435 to its maximum value of 12% at a ratio of tip speed 0.465, when tested at blade angle of 15° . It gives an increase of 6.0% in maximum power coefficient when compared with maximum value at blade angle of 10° . Finally, this configuration tested at blade angle of 20° with the sample wind velocity range, and it achieved a lower result than turbine model results tested at blade angle of 15° . It gives 8.6% maximum power coefficient against tip speed ratio of 0.462 as shown in Figure 7.

The power coefficient of turbine model tested with two blades against tip speed ratio characteristic results gave view of turbine model behavior and from that the level of power coefficient at every tip speed ratio and also the point of maximum value of power coefficient (C_{Pmax}) were obtained.

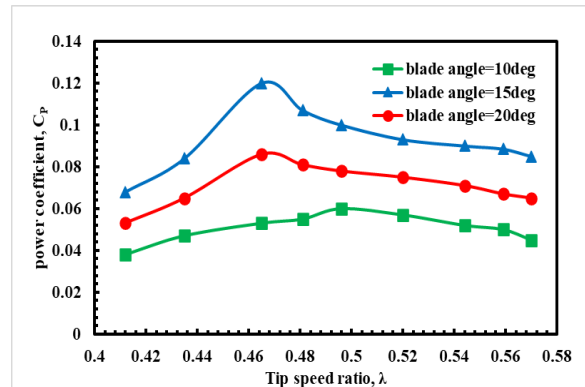


Figure 7: The relation between power coefficient and tip speed ratio for two-bladed turbine with blade angles of 10° , 15° , and 20° .

3.1.2 Configuration (B)

The overall 3-bladed turbine model performance, configuration (B) is presented in Figure 8, the torque coefficient (C_T) against tip-speed ratio (λ) characteristic of a tested 3-bladed turbine model without flaps is examined at three different blade angles (10° , 15° , 20°). The torque coefficient is defined as ratio measured

torque to calculated torque, and the tip speed ratio is defined blade tip speed to wind speed. At the blade angle of 10° , it is noticed that at a ratio of tip speed 0.518, the torque coefficient is 18.5%. With increasing in tip speed ratio, the torque coefficient increases until its maximum value of 23.0% against tip speed ratio of 0.556, then increase in tip speed ratio over 0.556 means decrease in torque coefficient.

When the 3-bladed model rotor tested at blade angle of 15° , the torque coefficient increased from 25.7% at tip-speed ratio, λ of 0.518 to its maximum value of 31.8% against tip-speed ratio of 0.575 as shown in Figure 8. It gives an improvement of 38.3% when compared with its results during testing at blade angle of 10° . Finally, this configuration tested at blade angle of 20° with the sample wind velocity range, and it achieved a lower result than turbine model results tested at blade angle of 15° . It gives 27.2% maximum torque coefficient against tip speed ratio of 0.575 as shown in Figure 8.

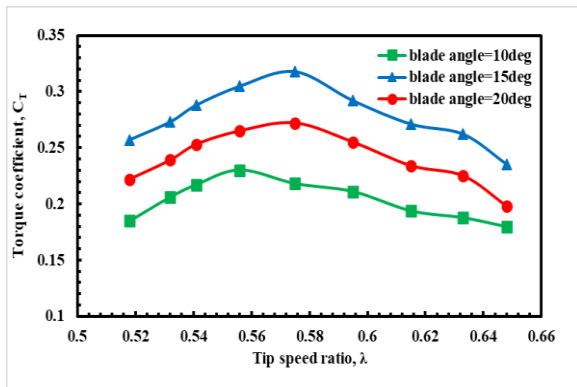


Figure 8: The relation between torque coefficient and tip speed ratio for three-bladed turbine with blade angles of 10° , 15° , and 20° .

The overall 3-bladed turbine model performance, configuration (B) is presented in Figure 9 the power coefficient (C_P) against tip-speed ratio (λ) characteristic of a tested 3-bladed turbine model without Flaps is examined at three different blade angles ($10^\circ, 15^\circ, 20^\circ$). It is noticed from Figure 9 the power coefficient (C_P) of the tested 3-bladed model at blade angle of 10° against tip speed ratio that the power coefficient increased from 9.0% at tip speed ratio of 0.518 to maximum value of 10.5% at tip speed ratio of 0.556 and then decreases with increasing in tip speed ratio. It is noticed that the power coefficient increased from 18.0% at tip-speed ratio of 0.518 to its maximum value of 23.0% at a ratio of tip speed 0.575, when tested at blade angle of 15° as shown in Figure 9. It gives an increase of 12.5% in maximum power coefficient when compared with maximum value

at blade angle of 10° . When this configuration tested with blade angle, 20° the power coefficient decreased at all values of tip speed ratio during this test when compared with its results at blade angle of 15° . It gave 17.2% maximum power coefficient against tip speed ratio of 0.556 as shown in Figure 9.

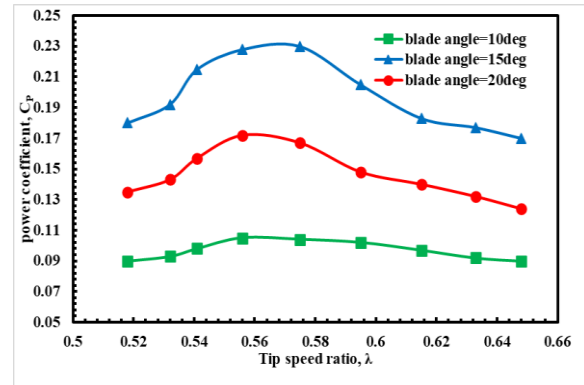


Figure 9: The relation between power coefficient and tip speed ratio for three-bladed turbine with blade angles of 10° , 15° , and 20° .

3.1.3 Configuration (C)

In this section the torque coefficient (C_T) against tip-speed ratio (λ) characteristic of a tested 6-bladed turbine model, configuration (C) without Flaps is examined at three different blade angles ($10^\circ, 15^\circ, 20^\circ$). Figure 10 shows the relation between torque coefficient, and tip speed ratio at blade angle of 10° , it is noticed that at tip speed ratio of 0.55, the torque coefficient is 53.1%. With increasing in tip speed ratio, the torque coefficient increases until its maximum value of 63.9% against the ratio of tip speed 0.65, then increase in tip speed ratio over 0.65 means decrease in torque coefficient.

When the 6-bladed model rotor, configuration(C) tested at blade angle of 15° , the torque coefficient increased from 62.2% at tip-speed ratio, λ of 0.55 to its maximum value of 73.2% against tip-speed ratio of 0.633 as shown in Figure 10. It gives an improvement of 14.5% when compared with its results during testing at blade angle of 10° . Finally, this configuration tested at blade angle of 20° with the sample wind velocity range, and it achieved a lower results than turbine model results tested at blade angle of 15° . It gave 66.7% maximum torque coefficient against tip speed ratio of 0.623 as shown in Figure 10. Increasing in blade angle from 15° to 20° means decreasing in torque coefficient for all value of tip speed ratio ranges in this experiment test.

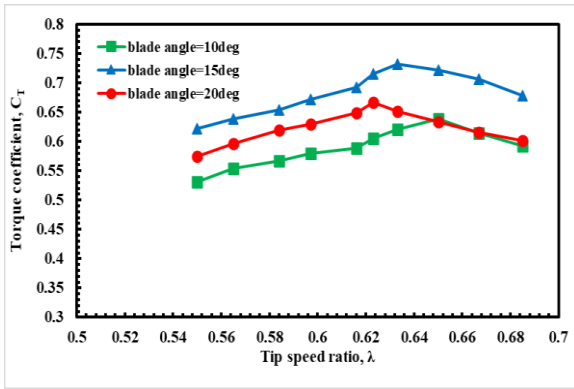


Figure 10: The relation between torque coefficient and tip speed ratio for six-bladed turbine with blade angles of 10°, 15°, and 20°.

Figure 11 shows the power coefficient (C_P) against the tip speed ratio for the 6-bladed model at different blade angles of 10°, 15°, and 20°. For the blade angle of 10° the power coefficient increased from 26.7% at tip speed ratio of 0.55 to maximum value of 39.0% at tip speed ratio of 0.65 and then decreases with increasing in tip speed ratio. It is also noticed that the power coefficient increased from 33.7% at a ratio of tip speed 0.55 to its maximum value of 44.7% at tip-speed ratio of 0.633, when tested at blade angle of 15° as shown in Figure 11. There is an increase of 14.6% in maximum power coefficient when compared with maximum value at blade angle of 10°. When this configuration is tested with blade angle of 20°, as shown in Figure 11. The power coefficient decreased at all values of tip speed ratio during this test when compared with it results at blade angle of 15°.

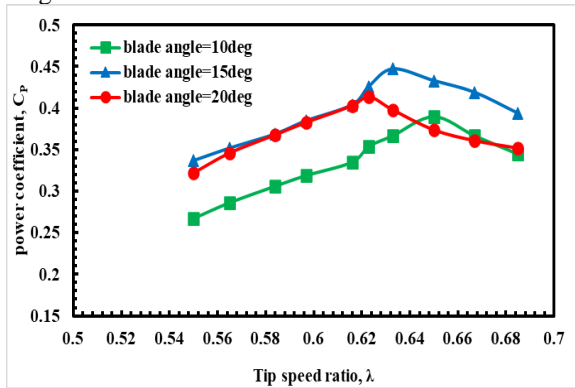


Figure 11: The relation between power coefficient and tip speed ratio for six-bladed turbine with blade angles of 10°, 15°, and 20°.

Comparison between three reference configurations (A, B, and C) tested at blade angle of 15° is plotted in

Figure 12. This figure shows the relation between torque coefficient, C_T , and the ratio of tip speed, λ , for 2-bladed, 3-bladed, and 6-bladed configurations tested at best angle in this experimental work.

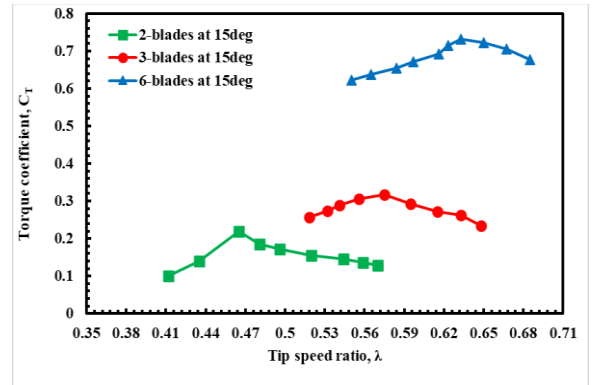


Figure 12: The relation between torque coefficient and tip speed ratio of two, three and six blades at 15°.

Figure 13 shows the relation between C_P , λ for configurations (A, B, and C) when tested at blade angle of 15°.

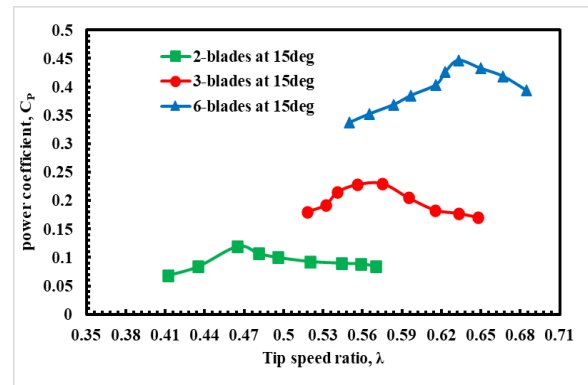


Figure 13: The relation between power coefficient and tip speed ratio for two, three and six-bladed turbine with blade angle 15°.

3.2 Configurations with Trailing Edge Flaps

In this section, the power coefficient versus tip speed ratio for the modified configurations tested with trailing edge flaps are presented. To have a direct comparison between the reference configuration results and the modified configuration, results were plotted on the same figure as the modified configuration. In addition, the coefficients from both reference configuration and modified configuration were plotted in the same way. Figure 14 shows the schematic position of the flap at different angles.

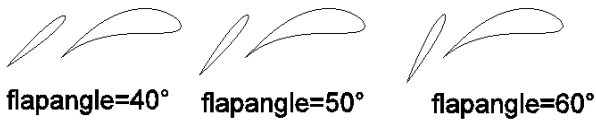


Figure 14: Schematic sketch of trailing edge flap at different angles.

Figure 15 shows the relation between power coefficient, C_p , and tip speed ratio, λ , for 3-bladed configuration with trailing edge flaps and without flap tested at the best blade angle (15°) occurred in this experimental work. In this section, the modified configuration tested at three values of flap blade angles (40° , 50° , and 60°). It is noticed that the modified configuration gave a good result when tested at flap angle of 50° , it achieved a maximum power coefficient of 35.8% at tip speed ratio of 0.835. It gave Improvement in max. Power coeff., $\Delta C_p = 55.6\%$.

$$\Delta C_p = [C_{p \max @ \beta = 15^\circ \text{ with flap at } 50^\circ} - C_{p \max @ \beta = 15^\circ \text{ without flap}}] / C_{p \max @ \beta = 15^\circ \text{ without flap}} \quad (11)$$

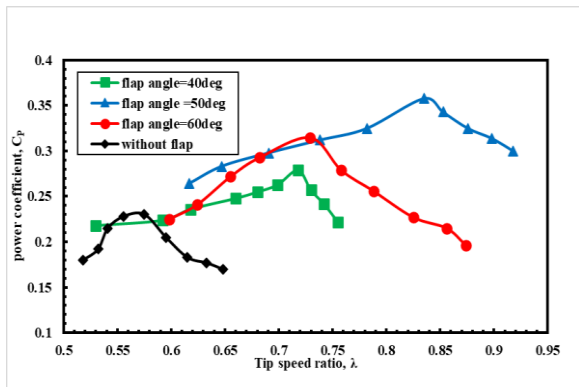


Figure 15: The relation between power coefficient and tip speed ratio for three bladed turbine with blade angle 15° without flap and with three different angles of flap 40° , 50° and 60° .

Figure 16 depicts the relation between power coefficient, C_p , and tip speed ratio, λ , for 6-bladed configuration with trailing edge flaps and without flap tested at the best blade angle (15°) occurred in this experimental work. In this section, the modified configuration tested at three values of flap blade angles (40° , 50° , and 60°). It is noticed that the modified configuration gave a good result when tested at flap angle of 50° , it achieved a maximum power coefficient of 55.7% at a ratio of tip speed 0.895. It gave Improvement in max. Power coeff., $\Delta C_p = 24.6\%$

$$\Delta C_p = [C_{p \max @ \beta = 15^\circ \text{ with flap at } 50^\circ} - C_{p \max @ \beta = 15^\circ \text{ without flap}}] / C_{p \max @ \beta = 15^\circ \text{ without flap}} \quad (12)$$

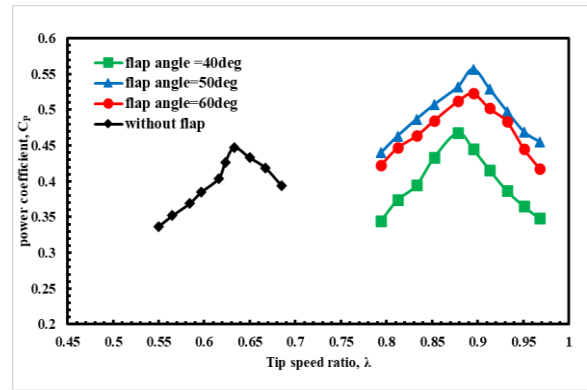


Figure 16: The relation between power coefficient and tip speed ratio for six- bladed turbine with blade angle 15° without flap and with three different angles of flap 40° , 50° and 60° .

4. CONCLUSIONS

This paper shows the result of an experimental investigation to study the effect of trailing edge Flap on the performance of a SHAWT at different number of blades and different blade and flap angles. Therefore, an experimental setup includes a model of wind turbine was constructed. The results revealed that:

1. For the blade angle, β , of 10° , 15° and 20° , without flaps and with two-bladed, three-bladed and six-bladed rotor, the blade angle of 15° is the best blade angle which gave 23% maximum power coefficient at three-bladed rotor and 44.7% maximum power coefficient at six-bladed rotor compared to that of the two-bladed rotor.
2. For the model tested with trailing edge flaps at flap angle, α , of 40° , 50° and 60° , the best setting angle of the flaps was 50° . With this angle, the model gave 35.8% maximum power coefficient with a three-bladed rotor and gave 55.7% maximum power coefficient with six- bladed rotor.
3. It was discovered that the use of trailing edge flaps can enhance the performance of horizontal axis wind turbines, with improvements in maximum power coefficient of 55% for three-bladed rotors compared to reference case that tested without any flaps and 24.6% for six-bladed rotors compared to reference case.

Statement of Authorship Contribution Credit

Author 1, performed experiments, literature research, data curation, writing an original draught, analysis, and result interpretation.

Author 2: supervision, methodology, validation, review & editing, analysis, and result interpretation.

Author 3: Editing, review, methodology, and supervision.

Author 4: Editing, review, methodology, and supervision.

Conflict of Interest Declaration

The authors reaffirm that none of their known financial or interpersonal conflicts appear to have affected the research reported in this paper.

5. REFERENCES

- [1] M. M. Elsakka, D. B. Ingham, L. Ma, and M. Pourkashanian, "Comparison of the Computational Fluid Dynamics Predictions of Vertical Axis Wind Turbine Performance Against Detailed Pressure Measurements," *Int. J. Renew. Energy Res.*, vol. 11, no. 1, pp. 276–293, 2021, doi: 10.20508/ijrer.v11i1.11755.g8131.
- [2] P. J. Schubel and R. J. Crossley, "Wind turbine blade design," *Energies*, vol. 5, no. 9, pp. 3425–3449, 2012, doi: 10.3390/en5093425.
- [3] S. Widiyanto, S. Pramonohadi, and M. K. Ridwan, "Performance Analysis of Small Horizontal Axis Wind Turbine with Airfoil NACA 4412," *Int. J. Sci. Technol. Manag.*, pp. 347–357, 2015.
- [4] A. Suresh and S. Rajakumar, "Design of small horizontal axis wind turbine for low wind speed rural applications," *Mater. Today Proc.*, vol. 23, pp. 16–22, 2019, doi: 10.1016/j.matpr.2019.06.008.
- [5] M. M. Ghorani, B. Karimi, S. M. Mirghavami, and Z. Saboohi, "A numerical study on the feasibility of electricity production using an optimized wind delivery system (Invelox) integrated with a Horizontal axis wind turbine (HAWT)," *Energy*, vol. 268, no. May 2022, p. 126643, 2023, doi: 10.1016/j.energy.2023.126643.
- [6] S. Iswahyudi, Sutrisno, Prajitno, and S. B. Wibowo, "Effect of blade tip shapes on the performance of a small HAWT: An investigation in a wind tunnel," *Case Stud. Therm. Eng.*, vol. 19, no. March, p. 100634, 2020, doi: 10.1016/j.csite.2020.100634.
- [7] H. R. Kaviani and A. Nejat, "Investigating the aeroelasticity effects on aeroacoustics and aerodynamics of a MW-class HAWT," *J. Wind Eng. Ind. Aerodyn.*, vol. 213, no. April, p. 104617, 2021, doi: 10.1016/j.jweia.2021.104617.
- [8] H. Bhavsar, S. Roy, and H. Niyas, "Multi-element airfoil configuration for HAWT: A novel slot design for improved aerodynamic performance," *Mater. Today Proc.*, vol. 72, pp. 386–393, 2023, doi: 10.1016/j.matpr.2022.08.110.
- [9] M. A. Shehata and A. A. Elmotalip, "Power Augmentation Due to Influence of Frontal and Rear Short Flaps on Performance of a Horizontal Axis Wind Turbine," pp. 1–12, 2000.
- [10] C. Zhuang, G. Yang, Y. Zhu, and D. Hu, "Effect of morphed trailing-edge flap on aerodynamic load control for a wind turbine blade section," *Renew. Energy*, vol. 148, pp. 964–974, 2020, doi: 10.1016/j.renene.2019.10.082.
- [11] Y. Zhang, V. Ramdoss, Z. Saleem, X. Wang, G. Schepers, and C. Ferreira, "Effects of root Gurney flaps on the aerodynamic performance of a horizontal axis wind turbine," *Energy*, vol. 187, p. 115955, 2019, doi: 10.1016/j.energy.2019.115955.
- [12] A. Mansi and D. Aydin, "The impact of trailing edge flap on the aerodynamic performance of small-scale horizontal axis wind turbine," *Energy Convers. Manag.*, vol. 256, no. February, p. 115396, 2022, doi: 10.1016/j.enconman.2022.115396.
- [13] X. Bofeng, F. Junheng, L. Qing, X. Chang, Z. Zhenzhou, and Y. Yue, "Aerodynamic performance analysis of a trailing-edge flap for wind turbines," *J. Phys. Conf. Ser.*, vol. 1037, no. 2, 2018, doi: 10.1088/1742-6596/1037/2/022020.